Evaluation of Defects in Seal Region of Food Packages Using the Backscattered Amplitude Integral (BAI) Technique

Ayhan Ozguler, Scott A. Morris, and William D. O'Brien, Jr.

A. Ozguler and S.A. Morris, Department of Food Science and Human Nutrition, University of Illinois, 1304 W. Pennsylvania Avenue, Urbana, IL 61801, W.D. O'Brien, Bioacoustics Research Laboratory, Department of Electrical and Computer Engineering, University of Illinois, 405 North Mathews Avenue, Urbana, IL 61801.

Abstract - The focus of this study is to evaluate the image contrast, denoted ΔBAI, for various packaging materials, and defect types and their sizes. This study applied the pulse-echo Backscattered Amplitude Integral (BAI) method to visualize and evaluate defects in the seal area of flexible food packages which might cause both economic loss and health hazards. This method yields an image, the BAI-mode image. It has been shown that there is a direct relation between the defect size and ΔBAI value, and that different defect types and packaging materials have a significant impact on the ΔBAI value.

I. INTRODUCTION

There are two major defects found in the seal region of flexible food packages: channel leaks and weak seals [1]. Channel leaks might cause a pathway for microbial penetration that eventually results in the spoilage of the product. The weak seal that is generally caused by wrinkles or product involvement in the seal area causes the seal strength to decrease, and that gives rise to product deterioration during storage [2]. Because both types of defects bring about health hazards and economic loss, it is imperative that packaging be checked for the presence of such defects.

A new technique called, Backscattered Amplitude Integral (BAI) method, which yields an image (the BAI-mode image) has been introduced for detection of small defects [3]. This technique has demonstrated the capability of detecting channel defects in the 10-μm range regardless of whether low impedance (air) or high impedance (water) material is present within the channel defect.

In this study, channel defects (air-filled and water-filled) in the range from 6 to 100 μm in diameter and inclusion defects in the range from 20 to 150 μm in diameter within the seal region of both plastic trilaminate and aluminum foil pouches were created in the laboratory. Mouse tail tendon as a simulation of typical biomaterial was used to generate inclusion defects. The purpose of this study is to evaluate the contrast descriptor, ΔBAI, for two packaging materials, three defect types and sizes.

II. METHODOLOGY

Sample Preparation

Microwaveable plastic (Fuji Tokushu Shigyo Co. Ltd., Seto Aichi, Japan) and aluminum foil trilaminate films were used for sample production. The thickness and sound speed for the transparent plastic film [4] were 110 μm and 2380 m/s, and those for the opaque aluminum foil film were 120 μm and 2460 m/s. Two types of defect were created, namely, channel and inclusion.

Smooth, die-drawn tungsten wires (California Fine Wire Company, Grover City, CA) with 6, 10, 15, 37, 50, 75 and 100 μm diameters were used to prepare channel defect. Mouse tail tendons (provided by Beckman Institute's Animal Care Facility, Urbana, IL) with 20-150 μm diameters were used to prepare inclusion defects. After the wire and the tendon were located between two layers of film, they were sealed into place by an automatic heat sealer (Doboy, HS-C42051, Doboy, Co., New Richmond, WI). The sealing temperature for plastic and aluminum foil was 132 and 152 °C, respectively. The longitudinal axis of wire and tendon was perpendicular to the sealing direction. The sample was left to cool for about 5 min following sealing. Air-filled channel defects were prepared by axially removing the wire after cooling. To prepare the water-filled channel defects, samples were immersed into the water bath, and the wire was axially removed. Next, both ends of channel opening and tendon were fused to assure the integrity of the

0-7803-4153-8/97/$10.00

defects' contents. Light transmission microscope was used to independently measure defects [3].

System Description and Data Acquisition

The sample was located in a water tank (~20°C) so that the defect orientation was approximately normal to the sound beam direction. A pulser-receiver (Model 5800, Panametrics, Waltham, MA) in pulse-echo mode was used with a spherical focused ultrasonic transducer (Panametrics V317, Waltham, MA), measured center frequency of 17.3 MHz. The Radio-Frequency (RF) echo signal from the pulser receiver was digitized (500Ms/s) using a LeCroy 9354TM (Chestnut, NY) oscilloscope.

The sample was scanned in a rectangular grid pattern by moving the transducer with an automatic micro-positioning system (Daedal, Inc., Harrison City, PA). The linear and rotational accuracy of the system are 2 μm and 0.01°, respectively. A host PC (486-66MHz) controlled the positioning system, pulser-receiver and oscilloscope, which were connected to GPIB-board. The distances between grids were 30 μm in the direction parallel to the seal direction (also transverse to the defect's longitudinal axis) and 100 μm in the direction perpendicular to the seal direction (30μm × 100 μm step sizes). Field-of-view varied from 1.5 mm × 1.0 mm to 2.0 mm × 4.0 mm area. Data were transferred to a SUN Sparc 20 workstation for off-line processing.

BAI-mode imaging

Each RF waveform was Hilbert-transformed, and the resulting envelope was integrated to obtain the BAI value for each point. The two-dimensional BAI-matrix was linearly interpolated by a factor of two in the sealing direction (30μm/2) and by a factor of seven transverse to sealing direction (100μm/7) yielding an image pixel size of 15.0μm × 14.3μm. The interpolated BAI matrix was normalized to produce a gray scale image, BAI-mode image [3]. All calculations were done by the built-in MATLAB® functions.

ΔBAI Contrast Descriptor

The ΔBAI contrast was calculated by

$$\Delta BAI = BAI_{background} - BAI_{defect} \quad (1)$$

where $BAI_{background}$ is the average BAI value of ten spatially separated locations from regions, which do not include the defect. BAI_{defect} is the average BAI value in the defect location. Fig. 1 indicates the reference region and defect location on the BAI-mode image. For calculation purposes, "*Imcrop*", built-in image processing function in MATLAB®, was used. Individual subimage areas were 0.3 mm × 0.3 mm, and ten different subimages were used to estimate the $BAI_{background}$ value. The same procedure was followed for the calculation of BAI_{defect}. However, only one subimage was selected which longitudinally covered the defect region (Fig. 1).

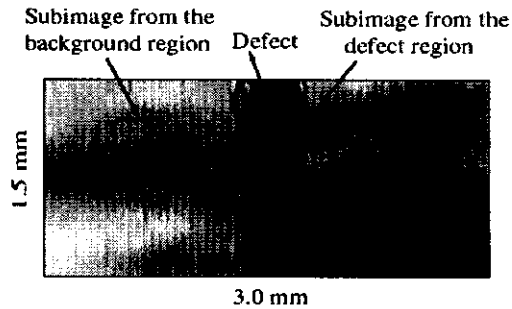

Figure 1: Normal incidence 17.3MHz BAI-mode image of water-filled channel defect (38μm) within the seal region of plastic pouch. ΔBAI was calculated from the region within the dashed rectangles

Statistical Analysis

Regression analysis between the size of defects and ΔBAI contrast values for each defect type was executed. In addition to this, one way ANOVA test (at a significance level of α=0.05) was performed to test if there was a difference between defect types and between packaging types in regard to ΔBAI contrast values. All of statistical calculations were performed by the built-in functions in Microsoft Excel® 97.

III. RESULTS & DISCUSSION

Channel defects were classified as: air-filled channel defect within plastic (ACP), water–filled channel defect within plastic (WCP), air-filled channel defect within aluminum foil (ACA), and water-filled channel defect within aluminum foil (WCA). Since seven different tungsten wires (6, 10, 15, 38, 50, 75, and 100 μm) were used to create these defects, and since five replications for each wire size were produced, thirty-five channel defects were fabricated for each group. Thus, a total of 140 channel defect samples were evaluated. Also, eighteen inclusion defects within plastic (IDP) and fifteen inclusion defects within aluminum foil (IDA) were evaluated.

The cross-sectional shape of almost all channel defects and tendons was elliptical. The major axis of the ellipse was in the direction parallel to the heat sealing direction. The major axis to minor axis ratio ranged from 0.88 to 1.76, and the mean and the standard deviation of this ratio were 1.16 ± 0.14 for channel defects. This ratio for tendons ranged from 1.02 to 3.72, and the mean and standard deviation of this ratio were 2.14 ± 0.81. The size measured in the major axis is the value quoted hereafter for the size of both channel and inclusion defects.

Fig. 2 shows the relationship between the ΔBAI value and defect size. The relationship of ΔBAI values with their respective defect sizes showed a linear correlation for each sample group. Table I indicates the slope of line-fit (defect size vs. ΔBAI) of raw data for each sample group and the corresponding correlation coefficient (R^2) obtained by the linear regression. The line-fit of each sample group in Fig. 2 was drawn according to results obtained by the regression analysis. High correlation coefficients clearly indicate that the ΔBAI contrast value decreased as the defect size decreased, i.e. BAI values in the defect region (BAI_{defect}) became close to those in the reference region ($BAI_{background}$) while the defect size declined.

According to ANOVA test at a significance level of α=0.05, ΔBAI values obtained for plastic samples were significantly lower than ($p<0.001$) those obtained for aluminum foil samples. Furthermore, the ΔBAI of water-filled channel defects (WCP) was higher than that of air-filled channel defects (ACP) within the seal region of plastic ($p=0.043$). On the contrary, the ΔBAI of water-filled channel defects (WCA) was lower than

Table I. Slope of line-fit (defect size vs. ΔBAI) for each sample group and correlation coefficients obtained from linear regression analysis ($p<0.001$ for each group).

Sample Group	Slope (V.s/m)	Correlation Coefficient (R^2)
ACP	0.233	0.91
WCP	0.250	0.89
ACA	0.359	0.88
WCA	0.317	0.91
IDP	0.124	0.79
IDA	0.081	0.75

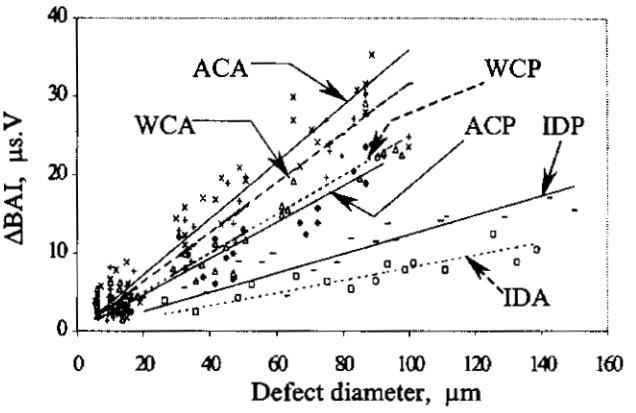

Figure 2: The size of defects vs. ΔBAI (×: ACA, +: WCA, △: WCP, ◆: ACP, -: IDP, □: IDA). The line-fit of each group was drawn according to its regression constants.

that of air-filled channel defects (ACA) within the seal region of aluminum foil ($p=0.033$). Moreover, the ΔBAI value of inclusion defects within the seal region of plastic was higher than that of aluminum foil ($p=0.012$). Fifteen samples from each group (IDA and IDP) were compared for this outcome. Consequently, the contrast descriptor, ΔBAI, varies with defect type, its size, and the material used for packaging.

The size of defects on the BAI-mode image is much larger than its actual size, and the same result was also supported by a recent study [3]. All channel defects (>15μm in diameter) were easily seen in the BAI-mode image. Even though as small as 6-μm channel defects could be detected by this technique, some small channel defects (≤15μm) were not identifiable, and the calculation of ΔBAI without knowing the exact location of the defect was impossible. A new technique in a recent study [6], which uses the same three-dimensional data set used in BAI-mode imaging, has the ability of detecting the small defects that BAI-mode imaging could not identify. This new high-contrast image technique looks like C-mode imaging. However, unlike conventional C-scan processing, which includes only a portion of the sample under investigation, the signal has been differently processed before processing the image (refer to [6]). After placing the image obtained by this technique and the BAI-mode image side by side, the location of the defect on the BAI-mode image was determined, and consequently,

ΔBAI contrast value of these unidentified samples, too, were calculated.

BAI-mode imaging technique has the capability of subwavelength detection of channel defects, e.g., detection of channel defects in sizes below 100 μm while λ (=c/f) for plastic is 138 μm and λ for aluminum foil is 142 μm at the center frequency of 17.3 MHz. In addition, all inclusion defects (20-150μm) prepared by the tendon were identified by this technique. Therefore, the BAI-mode imaging technique also has the capability of detecting small tendons down to 20μm. According to the several experts' opinion [1], detection of channel leaks as small as 50 μm in diameter by an in-line inspection system can provide an adequate safety assurance. In addition to that, the human visual inspection of such defects is mandated (U.S Code of Federal Regulations (9CFR§381.301(d) [5]), and human ocular resolution is approximately 50 μm. In that regard BAI-imaging technology already satisfies this regulation.

ΔBAI can be used in two means. First, the BAI-mode image itself is limited for characterizing the defect in terms of its size. However, by knowing the packaging material and by estimating what kind of defect might be involved to contaminate the seal region of the package, the size of the defect can be approximated using the calibration curve (ΔBAI vs. defect size). Different defects have a different impact on the ΔBAI value for the same packaging material. After recognizing all defect types within the seal region of a packaging material, the calibration curves would be prepared for each recognized defect type in the laboratory. Second, ΔBAI contrast descriptor on BAI-mode image can provide the safety requirement. After the minimum defect size is safely identified by BAI-mode image (15 μm in this study), the corresponding minimum ΔBAI contrast value can be set. This minimum value would provide a criteria whether the package is rejected from the inspection line or not, i.e., packages having a higher ΔBAI contrast value than the minimum requirement would be rejected from the inspection line. However, application of results in this study will require further research. The calculation of ΔBAI contrast descriptor requires manual data collection for the time being. A new technique, which recognizes the defect on the BAI-mode image and automatically calculates the ΔBAI contrast descriptor, is necessary for automation purposes.

ACKNOWLEDGEMENTS

The authors gratefully acknowledge the professional assistance with the sample validations by James F. Zachary, DVM, Ph.D., Department of Veterinary Pathobiology, University of Illinois. This work was supported in part by the Value-Added Research Opportunities Program, Agricultural Experiment Station, University of Illinois.

REFERENCES

[1] K.L Yam, "Pressure differential techniques for package integrity inspection," Ch. 17 in *Plastic Package Integrity Testing Assuring Seal Quality*, B.A. Blakistone and C.L Harper (Ed.), pp.137-145, Institute of Packaging Professionals, Herndon, VA, 1995.

[2] R.A. Lampi, G.L. Schulz, T. Ciavarani and P.T. Burke, " Performance and integrity of retort pouch seals," *Food Technology*, vol.30, no.2, pp.38-48, Feb. 1976.

[3] K. Raum, A. Ozguler, S.A. Morris, and W.D. O'Brien, Jr., "Channel defect detection in food packages using integrated backscatter ultrasound imaging," *IEEE Transactions on Ultrasonics, Ferroelectrics, and Frequency Control*, January 1998, (in press).

[4] A.A. Safvi, H.J. Meerbaum, S.A. Morris, C.L. Harper and W.D. O'Brien, Jr., "Acoustic imaging of defects in flexible food packages," Journal of Food Protection, vol.60, pp.309-314, Mar 1997.

[5] United States Code of Federal Regulations. Published by the Office of the Federal Register. Available from the superintendent of Documents, U.S. Government Print Office, Washington, DC 20402.

[6] C. H Frazier, A. Ozguler, S.A. Morris and W.D. O'Brien, Jr., "High-contrast images of defects in food package seals," IEEE 1997 Ultrasonics Symposium (document in this proceedings).